Aurora A Kinase Inhibition Is Synthetic Lethal with Loss of the *RB1* Tumor Suppressor Gene

Xueqian Gong[1], Jian Du[1], Stephen H. Parsons[1], Farhana F. Merzoug[1], Yue Webster[1], Philip W. Iversen[1], Li-Chun Chio[1], Robert D. Van Horn[1], Xi Lin[1], Wayne Blosser[1], Bomie Han[1], Shaoling Jin[1], Sufang Yao[1], Huimin Bian[1], Chris Ficklin[1], Li Fan[1], Avnish Kapoor[1], Stephen Antonysamy[2], Ann M. Mc Nulty[1], Karen Froning[2], Danalyn Manglicmot[2], Anna Pustilnik[2], Kenneth Weichert[2], Stephen R. Wasserman[3], Michele Dowless[1], Carlos Marugán[4], Carmen Baquero[4], María José Lallena[4], Scott W. Eastman[5], Yu-Hua Hui[1], Matthew Z. Dieter[1], Thompson Doman[1], Shaoyou Chu[1], Hui-Rong Qian[1], Xiang S. Ye[1], David A. Barda[1], Gregory D. Plowman[1], Christoph Reinhard[1], Robert M. Campbell[1], James R. Henry[1], and Sean G. Buchanan[1]

ABSTRACT

Loss-of-function mutations in the retinoblastoma gene *RB1* are common in several treatment-refractory cancers such as small-cell lung cancer and triple-negative breast cancer. To identify drugs synthetic lethal with *RB1* mutation (*RB1*^{mut}), we tested 36 cell-cycle inhibitors using a cancer cell panel profiling approach optimized to discern cytotoxic from cytostatic effects. Inhibitors of the Aurora kinases AURKA and AURKB showed the strongest *RB1* association in this assay. LY3295668, an AURKA inhibitor with over 1,000-fold selectivity versus AURKB, is distinguished by minimal toxicity to bone marrow cells at concentrations active against *RB1*^{mut} cancer cells and leads to durable regression of *RB1*^{mut} tumor xenografts at exposures that are well tolerated in rodents. Genetic suppression screens identified enforcers of the spindle-assembly checkpoint (SAC) as essential for LY3295668 cytotoxicity in RB1-deficient cancers and suggest a model in which a primed SAC creates a unique dependency on AURKA for mitotic exit and survival.

SIGNIFICANCE: The identification of a synthetic lethal interaction between *RB1* and AURKA inhibition, and the discovery of a drug that can be dosed continuously to achieve uninterrupted inhibition of AURKA kinase activity without myelosuppression, suggest a new approach for the treatment of RB1-deficient malignancies, including patients progressing on CDK4/6 inhibitors.

See related commentary by Dick and Li, p. 169.

[1]Eli Lilly and Company, Indianapolis, Indiana. [2]Eli Lilly and Company, Discovery Chemistry Research and Technologies, Lilly Biotechnology Center, San Diego, California. [3]Eli Lilly and Company, Advanced Photon Source, Argonne National Laboratory, Argonne, Illinois. [4]Eli Lilly and Company, Lilly Research Laboratories, Avenida de la Industria, Alcobendas, Spain. [5]Eli Lilly and Company, Alexandria Center for Life Sciences, New York, New York.

Note: Supplementary data for this article are available at Cancer Discovery Online (http://cancerdiscovery.aacrjournals.org/).

X. Gong, J. Du, and S.H. Parsons contributed equally to this work.

Corresponding Author: Sean G. Buchanan, Lilly Corporate Center, Indianapolis, IN 46285. Phone: 317-651-4187; E-mail: buchananse@lilly.com

doi: 10.1158/2159-8290.CD-18-0469

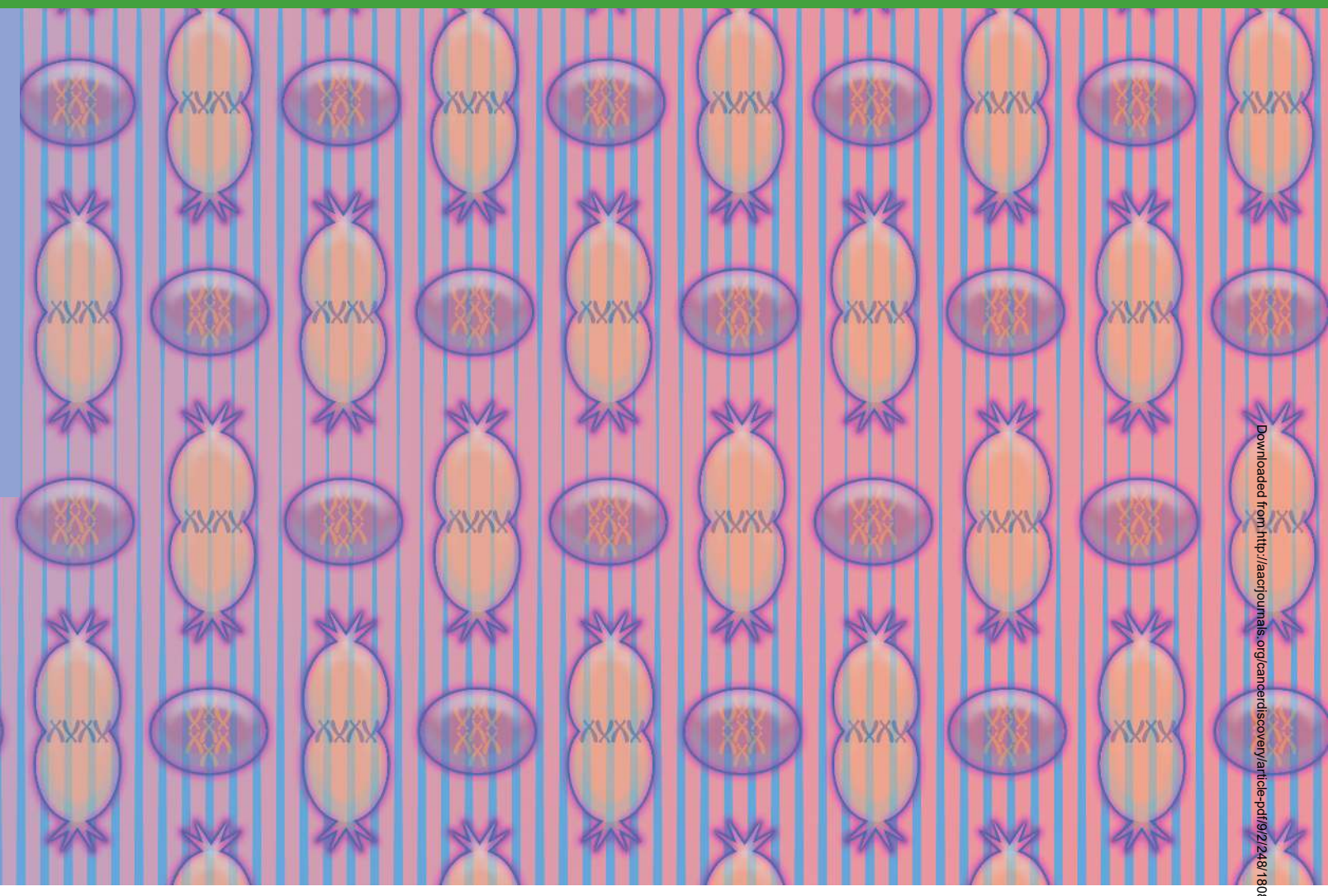

INTRODUCTION

An attractive strategy for cancer therapeutic discovery is to target enzyme functions that are dispensable in normal cells, but become essential for the survival of cells with mutated proto-oncogenes and tumor suppressor genes due to oncogene addiction (1), collateral vulnerability (2), and, more generally, synthetic lethality (3). Although numerous drugs that exploit oncogene addiction have proved successful for the treatment of cancer, mutated tumor suppressor genes (TSG) have thus far proved more challenging. A notable exception is the synthetic lethal interaction between *BRCA*-mutant cancer cells and PARP inhibitors, and it has been proposed that this example should encourage the search for synthetic lethal "gene–drug" interactions to target other TSGs in cancer (4).

One approach to the identification of new, synthetic lethal, gene–drug relationships is to perform genetic loss-of-function screens to identify dependencies, unique to cells with the mutated TSG, on genes that encode druggable enzymes (5). Drugs directed against the enzyme functions of hits from these screens must then be developed and tested to ensure that the gene–gene synthetic lethal relationship from the screen is preserved as a gene–drug interaction, not only in the screening models, but also, more broadly, among cells representing the clinical diversity of cancers with the TSG mutation. Indeed, depletion of a gene, or its mRNA (and therefore protein), as occurs in genetic screens, can have very different phenotypic consequences to inhibition of its encoded enzyme function with a drug, and examples of discrepancies between gene knockdown and enzyme inhibition are well known (6). Most importantly, genetic screens will miss genuine synthetic lethal relationships between a mutated cancer gene and enzyme blockade if the protein has additional functions, beyond the enzyme activity, which are essential to viability of all cells. Ultimately, of course, it is the "gene–drug" synthetic lethality that is required for therapeutic application, so an appealing alternative approach to "gene–gene" screens is to directly screen drug-like compounds across large panels of cancer cell lines to determine whether TSG-mutated cancers display enhanced vulnerability to particular drugs. Such gene–drug screens avoid many of the shortcomings of gene–gene screens but require that sufficiently specific, cell-active enzyme inhibitors against the relevant target already exist.

The prototypical TSG, retinoblastoma or *RB1*, is mutated in some of the most aggressive and hard-to-treat malignancies,

including small-cell lung cancer (SCLC) and triple-negative breast cancer (TNBC; ref. 7). The function of the *RB1* product, RB1, in controlling the G_1–S transition in the cell cycle is well understood (8). New cell cycles are triggered by mitogens and hormones that activate G_1 cyclins and these, in turn, promote the phosphorylation and neutralization of RB1. *RB1* loss, therefore, subverts the normal requirement for external growth cues, and cancers with *RB1* mutation are expected to be refractory to cancer therapeutics acting on upstream mitogen and hormone pathways. Indeed, *RB1* loss can emerge as a mechanism of resistance to EGFR, CDK4, and ER antagonists in lung (9) and breast (10, 11) cancers. In addition to its well-characterized role in controlling entry to S phase, multiple groups have reported that loss of RB1 leads to a hyperactivated or "primed" spindle-assembly checkpoint (SAC; ref. 12). These results imply that *RB1*-mutant cancer cells must rely on a mechanism to overcome SAC priming to avoid the fitness cost of stalled mitoses (13), but the basis of that mechanism remains unknown.

The antiproliferative activities of various cell-cycle inhibitors, as well as inhibitors of pathways that regulate RB1, such as the RAS–RAF pathway, have been linked to *RB1* status (14–17). However, none of these drugs have been developed specifically for *RB1*-mutant cancers. Cytotoxic chemotherapy regimens acting post G_1 in the cell cycle, e.g., tubulin-binding drugs, do have activity against $RB1^{mut}$ tumors (16). However, these drugs are indiscriminate (18) and are widely used to treat malignancies, such as hormone receptor–positive breast cancer, that are predominantly RB1-positive. Nevertheless, these results hint that *RB1* mutation may confer unique vulnerabilities at particular cell-cycle stages that could be exploited for the development of more effective treatments.

We previously reported a pharmacogenomic screening assay (19) that overcomes the confounding effects of the widely differing growth rates of human cancer cells (20). Importantly, as we show, this assay format permits uniform distinction between cytotoxic and cytostatic effects despite varying cell-cycle times and so is well suited to test drugs that act on the cell cycle for synthetic lethal interactions. Using this assay to find drugs toxic to $RB1^{mut}$ cancer, we identified inhibitors of Aurora kinases as top-scoring hits and demonstrate that LY3295668, a highly specific AURKA inhibitor, can kill RB1-deficient cancer cells at doses that have minimal effects on normal cells.

RESULTS

RB1-Mutant Cancer Cells Are Highly Sensitive to Aurora Kinase Inhibitors

In pharmacogenomic screens, the influence of cancer genomics on drug response is inferred from profiles of antiproliferative activity across large panels of cancer cell lines. This approach has been effective in uncovering associations between oncogenes that activate mitogenic signaling cascades and drugs that inhibit the same pathways (21, 22). However, the method has been less successful in identifying genetic associations for drugs that act directly on the cell cycle. This is surprising because many driver genes in cancer encode cell-cycle regulators, including frequently mutated TSGs such as *CDKN2A* and *RB1*. We were interested to tailor the conventional pharmacogenomics assay to cell-cycle inhibitors and to then test a collection of such compounds in parallel and determine which showed the most promising association to *RB1*.

We and others have previously shown that growth rate introduces substantial bias in the fixed duration (e.g., 72 hours) format that has been standard in pharmacogenomics assays (19, 20). Growth rate bias is expected to be particularly problematic for cell-cycle inhibitors and for distinguishing cytotoxic versus cytostatic effects. This is illustrated in the simulation in Supplementary Fig. S1, which shows how the dose–response curve of a cytostatic compound varies with the number of population doubling times (DT), converging after 3–4DT to resemble the curve of an otherwise equipotent cytotoxic compound. To overcome this artifact, we established the growth rates in vehicle control conditions for hundreds of genomically characterized cancer cell lines and developed a pharmacogenomic screening assay normalized for growth rate by running each assay for 2DT rather than for a fixed duration (19).

We then used our 2DT drug-screening assay to identify drugs selectively toxic to $RB1^{mut}$ cancer cells. Thirty-six inhibitors that act on the cell cycle, or cell-cycle regulating pathways, were selected for testing. These compounds inhibit a diversity of targets involved at all phases of the cell cycle with a bias toward drugs or drug-like compounds. The collection included compounds targeting G_1 to S phase regulators (e.g., CDK4/6), S phase processes (e.g., CDC7 and topoisomerase inhibitors), mitotic proteins (e.g., tubulin, PLK1, and Aurora kinases), mitogenic signaling pathways impacting G_1–S transition (e.g., RAS pathway, RSK1 and mTOR), and other proteins that have been shown to impact cell-cycle regulators such as MYC, $p21^{CIP1}$, and p53 (e.g., BRD4 and MDM2).

The antiproliferative activity of the 36 compounds against between 62 and over 500 cell lines from diverse epithelial, mesenchymal, and hematologic cancer lineages was determined (Supplementary Table S1). The test panel included, at minimum, 7 (range, 7–50) *RB1*-mutant cell lines to ensure sufficient power to detect *RB1* synthetic lethal relationships. We ranked the 36 compounds for the strength of the association of sensitivity to *RB1* mutation status using statistical methods described previously (19). As can be seen in Fig. 1A, *RB1* mutation associates with resistance to RAF, MEK, and CDK4/6 inhibitors and, conversely, to sensitivity to all three tested Aurora kinase inhibitors. $RB1^{mut}$ cells were, on average, also more sensitive than wild-type cells to inhibitors of other proteins active in mitosis, including the kinesin Eg5, and microtubules, but none of these compounds showed the same strength of association as the Aurora kinase inhibitors. This difference was not an artifact of the different number of cell lines tested for each drug because a similar relationship was derived from a common set of 443 cell lines that were tested with 12 of the compounds, including 7 different mitosis inhibitors (Supplementary Table S1). A weak preferential sensitivity of RB1-null cancers to inhibitors of p38, RSK, PLK1, Eg5, and microtubules has been described before (16). However, Aurora kinase inhibitors showed a much more pronounced effect than inhibitors of these targets in our profiling, suggesting that Aurora kinase inhibition might offer a unique therapeutic window that could be exploited for the treatment of *RB1*-mutant cancer. As explained below, we focused our

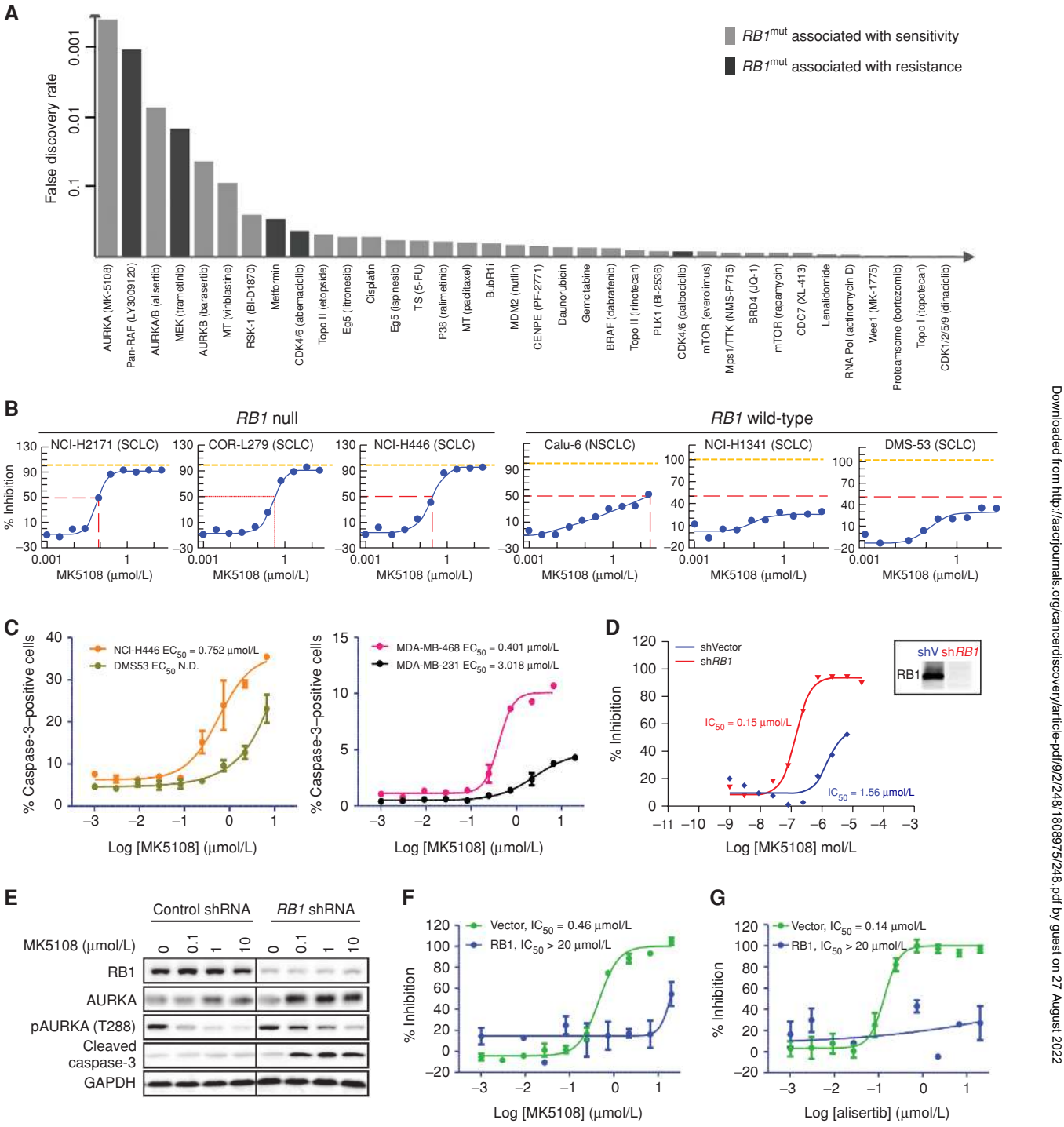

Figure 1. AURKAi are synthetic lethal with *RB1* loss. **A,** FDR statistic for association between *RB1* mutation and sensitivity (gray) or resistance (black) to 36 compounds (see Supplementary Table S1 for details). **B,** Dose–response curves from *RB1*-mutant and *RB1*–wild-type lung cancer cell lines treated with MK5108 using CellTiter-Glo (CTG). **C,** Caspase-3 activation in RB1-null (NCI-H446, MDA-MB-468) versus RB1$^+$ (DMS-53, MDA-MB-231) cell lines treated with MK5108 from at least 2 independent experiments. N.D., not determinable from data. **D,** MK5108 dose–response curves in Calu-6 (RB1$^+$, NSCLC) cells treated with shRNA directed at *RB1* or control (RB1 protein levels in the two conditions shown inset). **E,** Effect of *RB1* knockdown on MDA-MB-231 cells treated with MK5108. **F** and **G,** *RB1* was expressed in RB1-null MDA-MB-436 cells and their response to MK5108 (**F**) or alisertib (**G**) was tested using propidium iodide (PI) staining and high-content imaging in at least 2 independent experiments.

subsequent investigation on further characterizing the relationship between *RB1* status and response to Aurora A kinase inhibitors (AURKAi).

After 2DT, cell number will correspond to 25% of the DMSO control in response to the maximal effect of a purely cytostatic inhibitor. Therefore, we can infer that maximal inhibition values greater than 75% correspond to cytotoxic activity. As shown in Fig. 1B, the dose–response curves from the 2DT proliferation assay have a cytotoxic signature in *RB1*^{mut} cells, whereas a cytostatic signature typified *RB1* wild-type (*RB1*^{WT}) cells treated with the top-scoring drug from our screen, the AURKAi MK5108. This difference in effect is presumably due to increased apoptosis because caspase 3/7 activation was enhanced in RB1-null versus RB1^{+} lung and breast cancer cells (Fig. 1C), and is not explained by weaker inhibition of AURKA kinase activity in RB1^{+} cells (Supplementary Fig. S2A and S2B). Artificial depletion of RB1 from *RB1*^{WT} lung and breast cancer cells (using either shRNA or siRNA reagents) led to enhanced cytotoxicity in response to the AURKAi (Fig. 1D and E; Supplementary Fig. S3A and S3B), whereas ectopic *RB1* expression in RB1-null cells was protective (Fig. 1F and G). Altogether, these data indicate that our screening assay had, as intended, identified a synthetic lethal gene–drug interaction for *RB1*.

A similar, RB1-dependent, sensitivity to inhibitors of either AURKA or AURKB, as well as a synthetic lethal *RB1–AURKB* gene–gene interaction, is described in a companion paper in this issue by Oser and colleagues. Interestingly, *AURKA* gene knockout does not appear to associate strongly with *RB1* (or MYC family gene) status, presumably because it is an essential gene in mammalian cells (23–25). Consistent with this, we found that *AURKA* has the profile of a pan-dependent gene from a recently published, genome-wide CRISPR screening data set across 342 cancer cell lines (26) scoring as similarly critical for *RB1*^{mut} and *RB1*^{WT} cells (data not shown). This contrasts with the ability of *RB1*^{WT} cells to survive high concentrations of AURKA inhibitors, and exemplifies the commonly observed phenomenon of protein depletion having a more severe phenotype than enzyme blockade (6).

The Cytotoxicity of AURKAi in *RB1*-Mutant Cells Is Dependent on Inhibition of AURKA

In addition to alisertib, which inhibits both AURKA and AURKB (see below), both AURKA-dominant (MK5108 and MLN-8054) and AURKB-specific (barasertib) compounds showed a strong association with *RB1,* implying that inhibition of either Aurora kinase should be sufficient to achieve a synthetic lethality. Because myelosuppression has been encountered in clinical studies with AURKB-specific and dual AURKA/B inhibitors (27–29), but not AURKA-dominant drugs MK5108 and MLN-8054 (30, 31), we reasoned that specific inhibition of AURKA might be better tolerated than AURKB, resulting in a better therapeutic window and permitting a higher dose intensity to more effectively treat RB1-deficient cancers.

Crystal structures reveal several features that distinguish the active site of AURKA from AURKB, which we exploited to design a highly potent and selective inhibitor. The substituted isoquinoline (compound 1) derived from these efforts (Supplementary Fig. S4A and S4B). The carboxylic acid of compound 1 abuts Thr217 in AURKA but is sterically and electronically incompatible with the glutamate at the equivalent position in AURKB. The methylated piperidine ring likely further increases potency toward AURKA by establishing a novel water-mediated hydrogen bond to the main-chain carbonyl of Glu260. Compound 1 potently inhibited AURKA autophosphorylation (0.46 nmol/L IC_{50}) in *RB1*^{mut} NCI-H446 cells with over 1,000-fold selectivity against AURKB (measured by inhibition of phospho-histone H3). Capitalizing on these observations, further optimization of compound 1 led to the discovery of LY3295668 (Fig. 2A and B; Supplementary Information), an orally active compound with greater selectivity over AURKB than any Aurora inhibitor reported to date (Fig. 2C, and further described in a manuscript under review, J.D., R.C., J.H.). The fluorine atom on the pyridine ring of LY3295668 helps orient the carboxylate in LY3295668 closer to Thr217 of AURKA, likely contributing to its increased selectivity over AURKB. (AURKC is also more than 2 orders of magnitude less sensitive to LY3295668 than AURKA in enzyme assays; data not shown.)

Because the Aurora kinase inhibitors tested in our original screen are not exquisitely specific for AURKA (Fig. 2C; ref. 32), we wanted to determine whether LY3295668 maintained the strong association with *RB1* status observed for those drugs across our cell line panel using the 2DT assay. (As shown in Supplementary Fig. S5, there was no correlation between cell line sensitivity and growth rate, suggesting that, as anticipated, the 2DT format counteracts growth rate bias.) Across 517 cancer cell lines, those most sensitive to LY3295668 included *RB1*^{mut} lung cancer, breast cancer, myeloma, retinoblastoma, and glioblastoma (Supplementary Table S2; Supplementary Fig. S6), and *RB1* was the mutation most significantly associated with response to LY3295668 (Fig. 3A). The statistic for *RB1* association is best powered in lung and breast cancer cells (Supplementary Fig. S6), so we focused the remainder of our investigation on these tumor types. Like MK5108, LY3295668 gave cytotoxic profiles in RB1-null, but not RB1^{+}, SCLC cells, and in RB1^{+} NSCLC cells depleted of *RB1* by shRNA (Fig. 3B and C), and activated apoptosis pathways much more strongly in RB1-null versus RB1^{+} lung and breast cancer cell lines (Fig. 3D and E; Supplementary Fig. S7). These data confirm that AURKAi-*RB1* synthetic lethality does not require AURKB inhibition.

To complement studies in which *RB1* is artificially depleted from cancer cells, we also examined the consequence of natural loss of RB1 as an adaptive response to selective pressure from drug treatment during acquired resistance (14). We took two CDK4/6i-sensitive ER^{+} breast cancer cell lines, MCF7 and MDA-MB-361, and from each derived palbociclib-resistant variants by prolonged drug selection (see Methods). Two independent, palbociclib-resistant variants of MDA-MB-361 cells were generated, one (MB-361-PR) from a conventional, rising dose selection method, the other (MB-361-PRENU) from a protocol using a pretreatment with the mutagen ENU and then selecting a resistant clone at a fixed, high drug concentration (33). The two palbociclib-resistant variants of MDA-MB-361 cells exhibited reduced RB1 expression and dramatically enhanced sensitivity to AURKAi, whereas the drug-resistant MCF7 variant had higher levels of RB1, and was not sensitized to LY3295668 (Fig. 3F). By CRISPR-mediated removal of *RB1* from MDA-MB-361 cells, we confirmed that depletion of RB1 confers resistance to the CDK4/6i but sensitizes to LY3295668-induced apoptosis (Supplementary Fig. S8A–S8C).

A

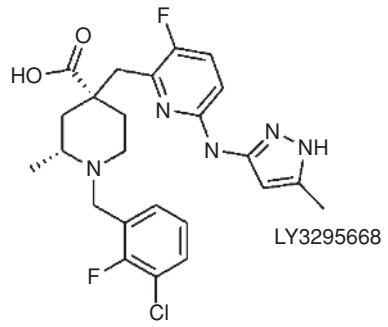

B

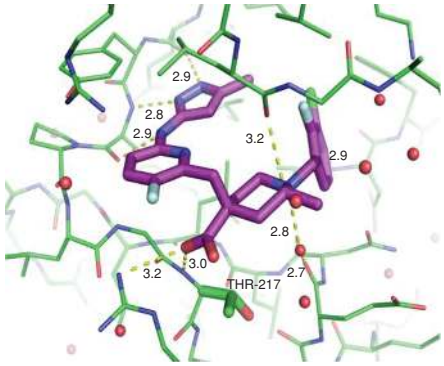

C

Compound	AURKA K_i (nmol/L)	AURKB K_i (nmol/L)	AURKA cell (H446 AURKA auto-P IC_{50}) (nmol/L)	AURKB cell (H446 pH3 inh 1 h IC_{50}) (nmol/L)	B/A cell ratio
MK5108	<0.81 (>0.037, *n* = 2)	4.7 (1.03, *n* = 2)	8 (3, *n* = 3)	4,210 (320, *n* = 2)	526
Alisertib	<1.1 (>0.21, *n* = 5)	5.8 (0.80, *n* = 6)	4 (2, *n* = 5)	51 (7, *n* = 2)	13
Barasertib	61 (19, *n* = 3)	2.8 (0.96, *n* = 3)	>10,930 (>7,000, *n* = 2)	11 (2, *n* = 11)	<0.001
Compound 1	<0.9 (>0.073, *n* = 7)	76 (13, *n* = 6)	<0.4 (>0.1, *n* = 10)	634 (84, *n* = 7)	>1,500
LY3295668	0.8 (0.066, *n* = 4)	1,038 (265, *n* = 5)	0.6 (0.5, *n* = 4)	1,420 (240, *n* = 4)	2,370

Figure 2. LY3295668 is a highly specific AURKA inhibitor. **A,** Chemical structure of LY3295668. **B,** X-ray structure of AURKA in complex with LY3295668 (magenta) determined at 2.0 Å. **C,** Geometric mean K_i or IC_{50} values (SEM, number of experiments) from enzyme and cell-based assays for Aurora inhibitors (inh) used in this study. In some experiments, values were undefined (below or above the threshold of detection, i.e., <1 or >10,000 nmol/L), and for these cases geometric mean and SEM values are listed as a minimum or maximum values.

Aberrations in cyclin-D and MYC family genes, which, like *RB1* loss, release E2F-driven transcription at the G_1–S cell-cycle checkpoint (34), were also strongly associated with the LY3295668 profile. A relationship between MYC and AURKAi sensitivity has been described previously (35, 36), and the sensitivities of 87 cancer cell lines to a dual AURKA/B inhibitor were linked to MYC genes using an assay format partially adjusted for growth rate (37). MYC family gene amplification and *RB1* mutation commonly co-occur, especially in SCLC. In the prior study across a small panel of cancer cell lines (37), all SCLC cell lines were *RB1* mutant, precluding isolation of *RB1* from MYC effects. In our profiling, although SCLC cells bearing both MYC family and *RB1* aberrations are more sensitive than SCLC with either feature alone, neither amplification nor high expression of MYC family genes is required for sensitivity of *RB1*-mutant cells: Several highly sensitive *RB1*-mutant cell lines have normal copy number and expression of MYC genes (Supplementary Fig. S9A and S9B). Furthermore, among *RB1*-mutant cancer cells, expression levels of MYC family genes do not correlate with Abs IC_{50} (Supplementary Fig. S10A). Interestingly, among cells with amplification of one of the MYC genes, most (10/11) of those with low *RB1* expression are sensitive whereas those expressing *RB1* have only about a 30% chance of being sensitive (Supplementary Fig. S10B). We also examined the AURKA-activating cofactors TACC3 and TPX2 to see whether their expression distinguished $RB1^{mut}$ from RB^{WT} cells. As shown in Supplementary Fig. S11A and S11B, there is no significant difference in expression of either cofactor in $RB1^{mut}$ cells.

The specificity of LY3295668 helped establish AURKA as the target most likely responsible for the *RB1* association. In a kinome-wide survey, only 5 of 386 kinases were potently inhibited by LY3295668 (<10 nmol/L; manuscript under review, J.D., R.C., J.H.), and none of these kinases overlapped with targets of the other AURKAi (MK5108, alisertib) that showed an *RB1* association. Notably, no inhibition of SYK, which has been reported essential in the context of RB1 loss (38), was observed up to 20 μmol/L. We verified that there is minimal SYK inhibition, relative to the IC_{50} for AURKA, for the different AURKAi. The AURKA IC_{50} is approximately 4,000-fold, 12,000-fold, or 50,000-fold lower than the SYK IC_{50} for MK5018, alisertib, and LY3295668, respectively (Supplementary Fig. S12). Conversely, the relatively potent inhibition of AURKA observed with the SYK inhibitor R406 (87 nmol/L AURKA vs. 42 nmol/L SYK) may contribute to the activity of R406 in retinoblastoma (38).

We reasoned that if AURKA was indeed the critical target for the toxicity of LY3295668 toward $RB1^{mut}$ cells, then a drug-binding defective form of AURKA would be able to rescue $RB1^{mut}$ cells from LY3295668 treatment. Our

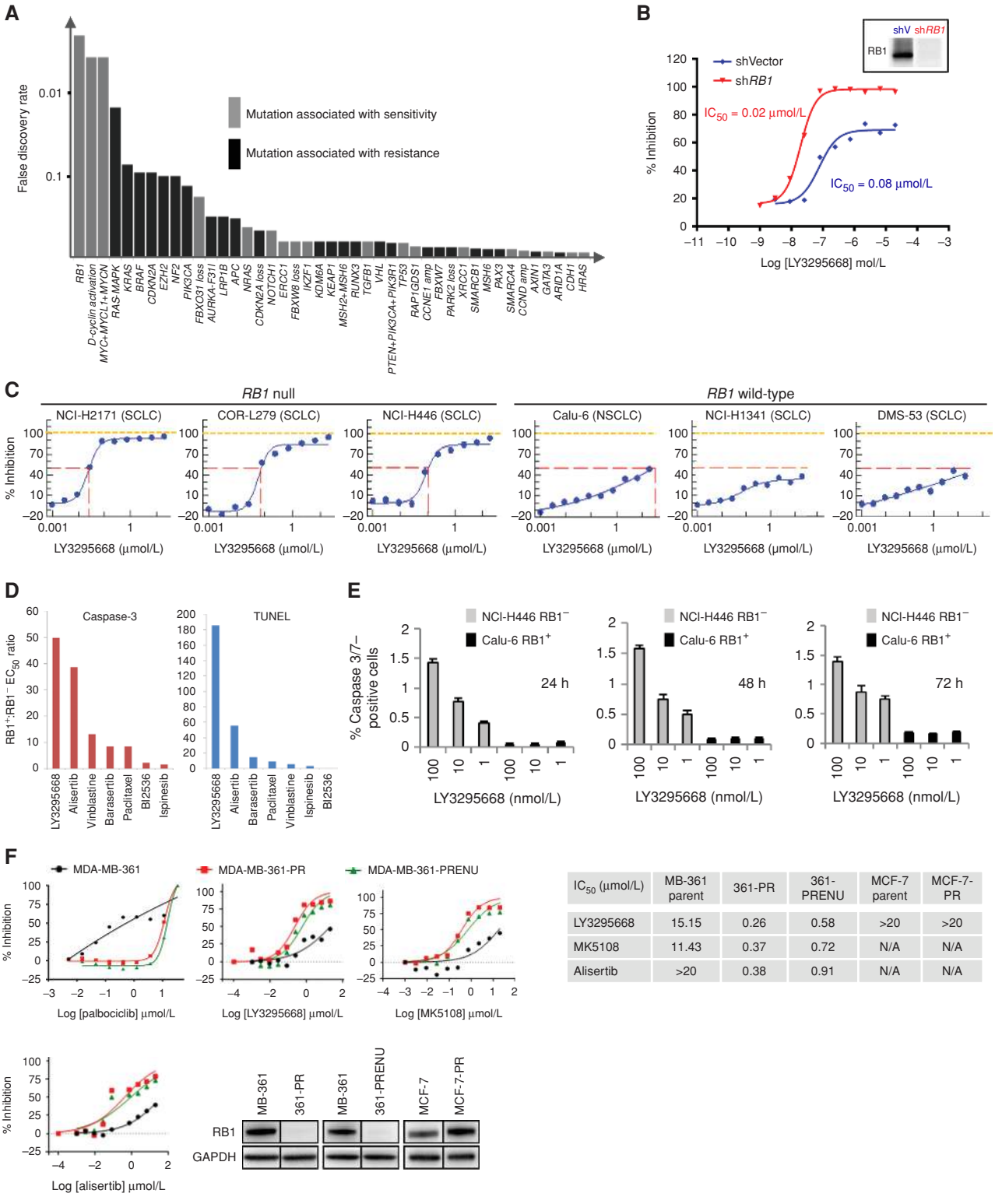

IC50 (µmol/L)	MB-361 parent	361-PR	361-PRENU	MCF-7 parent	MCF-7-PR
LY3295668	15.15	0.26	0.58	>20	>20
MK5108	11.43	0.37	0.72	N/A	N/A
Alisertib	>20	0.38	0.91	N/A	N/A

Figure 3. *RB1* synthetic lethality is retained by the highly AURKA-specific LY3295668. **A,** Top-scoring associations between LY3295668 Abs IC_{50} and key cancer genetic events across a panel of 517 human cancer cell lines from Supplementary Table S2. **B,** Representative dose–response curves from 2 independent experiments for LY3295668-treated Calu-6 ($RB1^+$, NSCLC) cells transfected with sh*RB1* or control shRNA. The percentage of inhibition from PI staining as described in Methods. **C,** LY3295668 dose–response curves in SCLC cell lines (CTG, 2DT). **D,** Ratio of average LY3295668 EC_{50} values for caspase-3 or TUNEL activation in $RB1^+$ (DMS-53, MDA-MB-231) versus RB1-null (NCI-H446, MDA-MB-468) cells from high content imaging from 2 independent experiments. **E,** Caspase 3/7 activation by LY3295668 from cell imaging (IncuCyte). $n = 2$ independent experiments. **F,** Antiproliferative effects (CTG, 2DT) of AURKAi against parent and palbociclib-resistant (PR) MDA-MB-361 and MCF-7 cells (representative curves from 3 independent experiments).

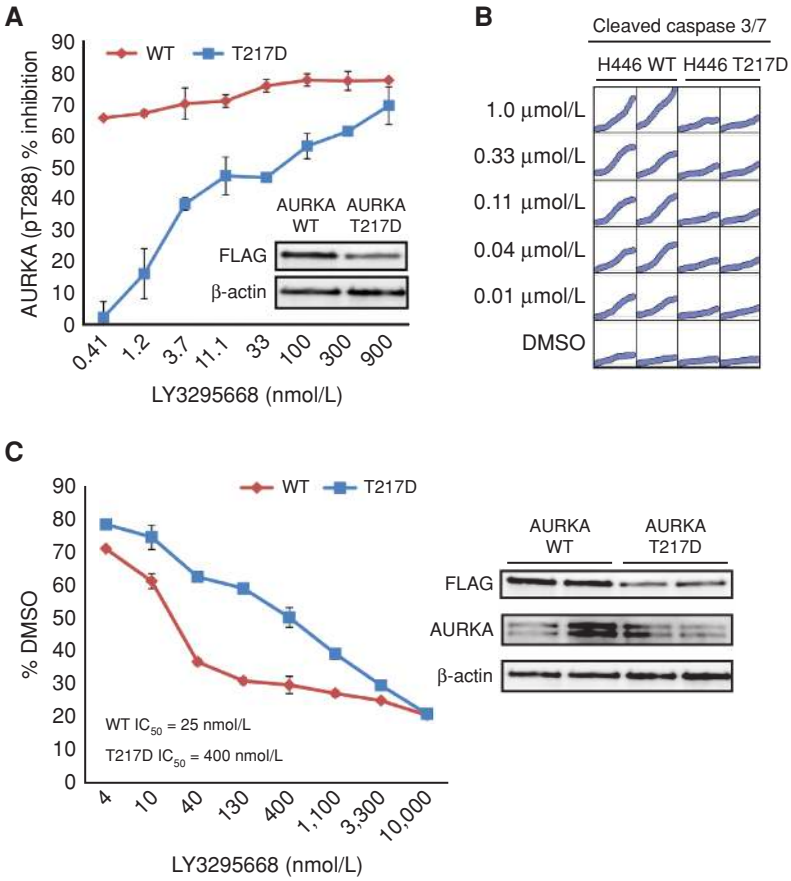

Figure 4. *RB1* synthetic lethality requires AURKA inhibition. Effect of LY3295668 on AURKA-pThr288 (**A**), caspase-3 cleavage (IncuCyte, **B**), and growth (CT96, **C**) in NCI-H446 cells expressing AURKA^{WT} (red) or AURKA^{Thr217Asp} (blue) from 2 independent experiments.

crystallography experiments had demonstrated that Thr217 is critical for high-affinity binding of LY3295668, so we expressed AURKA^{T217D} in *RB1*^{mut} H446 cells to determine whether AURKA inhibition is required for the drug's activity. AURKA^{T217D} is, as predicted, resistant to LY3295668 because cells expressing AURKA^{T217D} are resistant to inhibition of AURKA autophosphorylation (Fig. 4A). *RB1*^{mut} H446 cells expressing AURKA^{T217D} are also protected from the cytotoxicity of LY3295668 (Fig. 4B and C), demonstrating that AURKA inhibition is indeed critical for *RB1*-LY3295668 synthetic lethality.

LY3295668 Is Cytotoxic to *RB1*-Mutant Cancers at Exposures That Are Well Tolerated in Rodents and by Human Bone Marrow Cells

Assays to measure the cytotoxicity of drugs to human bone marrow (BM) cells growing *in vitro* are widely used for understanding the risk for clinical myelosuppression because they have a good track record of predictive power (39). Therefore, to test our hypothesis that truly specific AURKA inhibitors might avoid the myelosuppression seen with AURKB inhibitors, we tested the antiproliferative activity of LY3295668, and other Aurora kinase and mitosis inhibitors, toward human blood mononuclear cells to compare the relative cytotoxicity to BM versus *RB1*-mutant cancer cells. As shown in Fig. 5A, BM cells were 10-fold less sensitive to LY3295668 than *RB1*^{mut} H446 SCLC cells. In contrast, other mitotic inhibitors were toxic to BM cells at similar or even lower concentrations than those required to inhibit RB1-null cancer cells (Fig. 5A).

These data encouraged us to examine the efficacy of LY3295668 against SCLC tumors growing *in vivo*. Mice bearing SCLC xenografts were administered twice-daily doses of 50 mg/kg LY3295668 by oral gavage continuously for at least 3 weeks as shown in Fig. 5B. In accord with the *in vitro* findings, clear evidence of regression was observed for the three RB1-null SCLC xenograft models, but not for the *RB1*^{WT} PDX model LXFS-1129. The oncolytic activity of LY3295668 toward RB1-null tumors was rapid and persistent, provided the drug was continuously administered (Fig. 5B). The dosing regimen of LY3295668 used was chosen because it is well tolerated in mice and corresponds to plasma concentrations that exceed the IC_{90} for inhibition of AURKA for the entire dosing interval yet does not reach the IC_{90} for inhibition of AURKB, even at C_{max} (Fig. 5C). Similar exposures of LY3295668 in rats had insignificant toxicologic effects on BM cells. In a 1-month toxicology study, continuous dosing that resulted in comparable steady-state plasma concentrations to the mouse xenograft experiments caused no histologic changes in BM of the femur and sternum, and caused minimal changes in absolute numbers of circulating red blood cells, total white blood cells, lymphocytes, and eosinophils, with no effect on reticulocytes, platelets, neutrophils, or monocytes (data not shown).

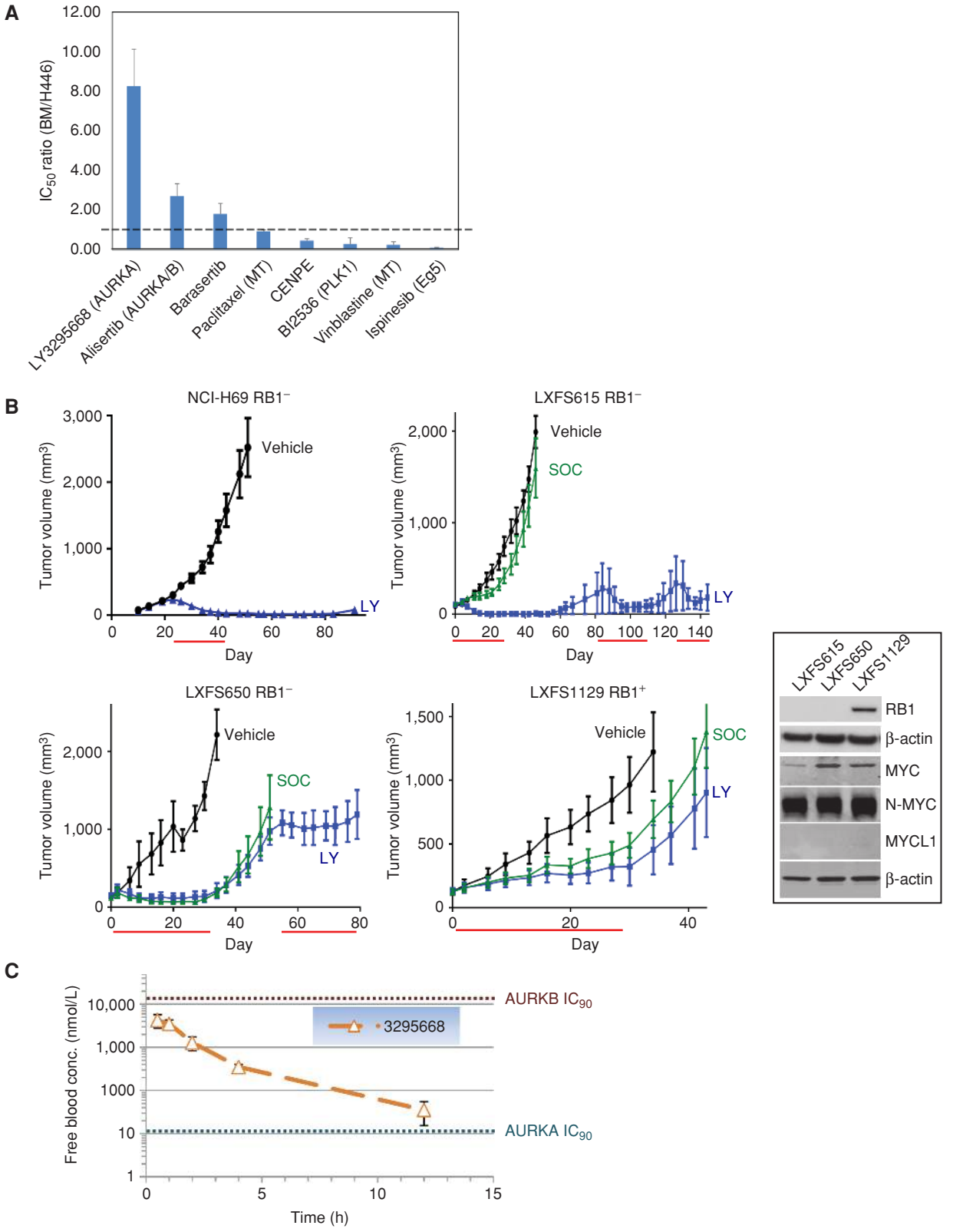

Figure 5. RB1-null SCLC tumor xenografts regress in response to well-tolerated concentrations of LY3295668. **A,** IC_{50} ratios (CTG) for human BM cells versus RB1-null NCI-H446 after 48 hours from 2 independent experiments **B,** Effect of LY3295668 (50 mg/Kg b.i.d. p.o.; blue) on growth of SCLC tumor xenografts versus standard-of-care (SOC; green). The dosing duration is indicated by the red line. RB1 expression levels in the PDX models inset. **C,** LY3295668 mean-free blood concentration in mice treated with LY3295668 50 mg/kg b.i.d. p.o. relative to the IC_{90} concentrations for AURKA or AURKB.

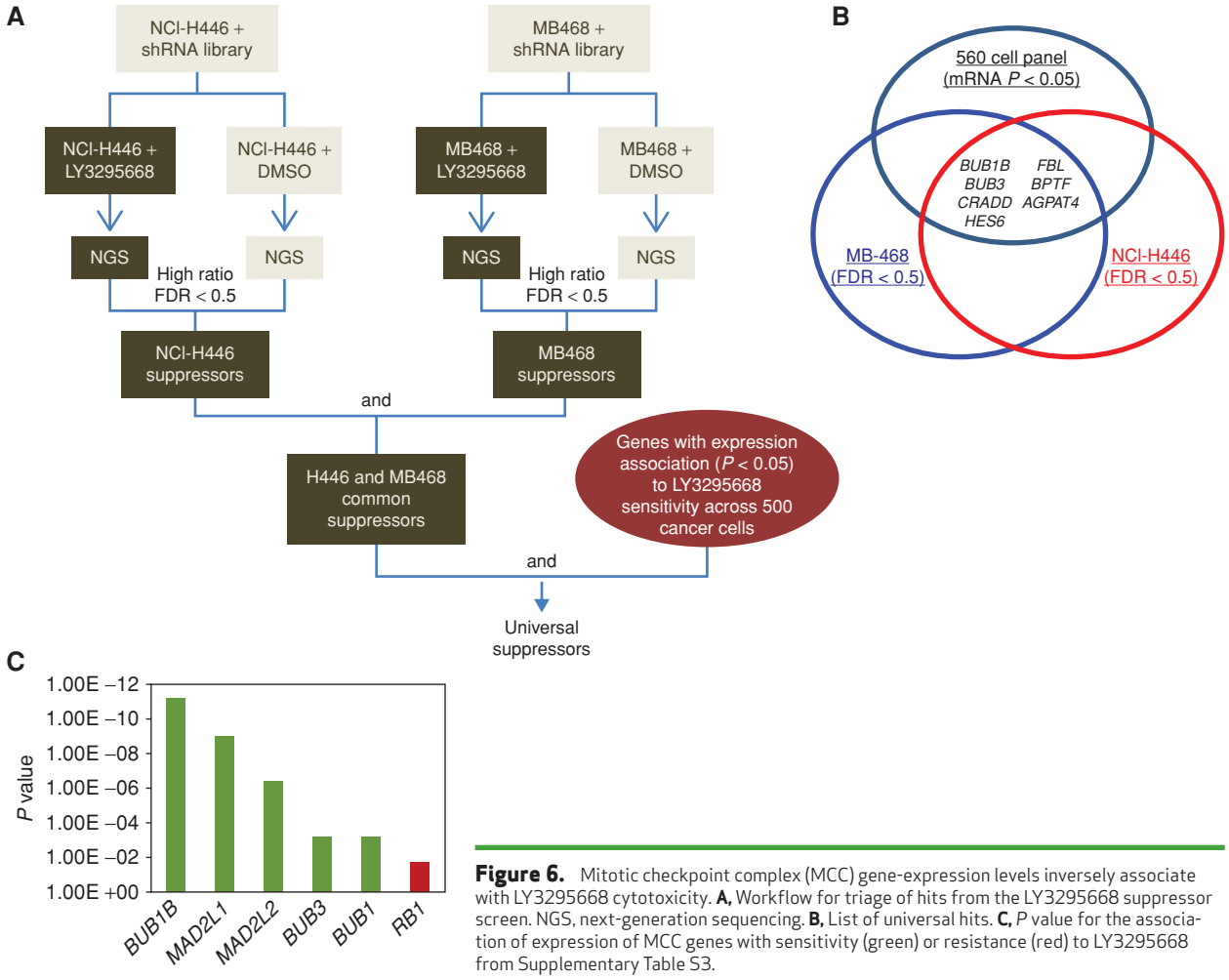

Figure 6. Mitotic checkpoint complex (MCC) gene-expression levels inversely associate with LY3295668 cytotoxicity. **A,** Workflow for triage of hits from the LY3295668 suppressor screen. NGS, next-generation sequencing. **B,** List of universal hits. **C,** *P* value for the association of expression of MCC genes with sensitivity (green) or resistance (red) to LY3295668 from Supplementary Table S3.

Intact SAC Function Is Required for the Cytotoxicity of LY3295668

Various functions have been ascribed to AURKA, the best-characterized being roles in orchestrating normal centrosome maturation and mitotic spindle assembly. In an effort to understand why *RB1*^{mut} cells are so highly dependent on AURKA, we examined whether LY3295668 has different effects on the morphology of the mitotic apparatus in *RB1*^{mut} compared with *RB1*^{WT} cells. These experiments are somewhat confounded by the rapid apoptosis apparent in RB1-null cells, but we saw no obvious differences in the effects of LY3295668 on centrosome biogenesis and mitotic spindle assembly in RB1-positive DMS-53 and MDA-MB-231 cells compared with RB1-null H2228 and HeLa cells (see below; data not shown).

These results hinted that a different function of AURKA may be responsible for the RB1 interaction. We reasoned that depletion of gene products critical for the sensitivity of *RB1*^{mut} cells to AURKAi would rescue cell growth in the presence of drug, and hence an unbiased genetic suppressor screen might give clues to the mechanistic basis of the *RB1*-AURKAi synthetic lethality. To this end, we used a genome-scale shRNA drug suppressor screen (40) in two RB1-null cells, NCI-H446 and MDA-MB-468, to identify genes critical for LY3295668 cytotoxicity (Supplementary Table S3). Several hits were identified, many common to both cell lines and therefore more likely true positives. These common suppressors might include both universal mechanisms that would explain the *RB1*-AURKAi pattern observed across our cell panel, as well as less general mechanisms restricted to these two cell lines. If depletion of a gene reduces sensitivity to AURKAi as a general mechanism, then cell lines with naturally low levels of the gene's transcript might be expected to be less sensitive to AURKAi across our cancer cell panel. Therefore, to enrich screening hits for genuine and broadly relevant suppressors, we triaged for genes where low mRNA associates with less sensitivity to LY3295668 across our entire cell line panel. We defined "universal suppressors" as genes whose expression (i) scores as required for sensitivity to LY3295668 in both NCI-H446 and MDA-MB-468 suppressor screens [false discovery rate (FDR) < 0.5] and (ii) associates with LY3295668 sensitivity in the pharmacogenomic cancer cell panel screen ($P < 0.05$; Fig. 6A; Supplementary Table S3). Seven genes meet these criteria (Fig. 6B) and include *BUB1B* and *BUB3*, two of the three mitotic checkpoint complex (MCC) genes responsible for enforcing the SAC by inhibiting the activity of the

anaphase promoting complex/cyclosome (APC/C). APC/C is the ubiquitin ligase responsible for degradation of securin and cyclin B to permit anaphase progression and mitotic exit (41). The third MCC gene, *MAD2L1*, was not represented in our shRNA library, but expression of *MAD2L1* also correlates very well with sensitivity to LY3295668 across the panel (Fig. 6C).

The link with MCC genes is notable because RB1 loss can prime expression of *BUB1B/MAD2L1* (42, 43), and it has been argued that RB1-null cancer cells must, therefore, acquire a mechanism to overcome the primed SAC and its negative impact on fitness (13). To explain our combined results, we wondered whether AURKA kinase activity, which, uniquely among the mitotic drug targets, is capable of overriding the SAC (44, 45), could contribute to this mechanism. If so, RB1-negative cells would be strictly dependent on AURKA activity to exit mitosis. This model predicts a profound mitotic arrest in RB1-null cells exposed to AURKAi concentrations that have minimal effect on mitotic duration in RB1-positive cells. AURKAi have been shown to cause a transient mitotic arrest in RB1-proficient cells, but this is typically readily resolved (46). In contrast, and consistent with this model, we find that in *RB1*^{mut} cells, LY3295668 prolongs the stability of the APC/C substrate cyclin B1 (Supplementary Fig. S13A–S13E) and causes a substantial mitotic arrest (Fig. 7A), without any evidence of AURKB inhibition and without obviously different consequences to the mitotic spindle morphology in *RB1*^{mut} versus *RB*^{WT} cells (Supplementary Figs. S13 and S14). The timing of apoptosis coincides with the mitotic arrest (Supplementary Fig. S13E), suggesting that AURKAi-treated RB1-null cells predominantly die as a consequence of failure to escape mitosis. Depletion of *BUB1B* (Fig. 7B) or *MAD2L1* (data not shown) reverses these effects, diminishing cyclin B1 accumulation and other markers of mitotic block, and reducing apoptosis. The enhanced LY3295668 sensitivity of breast and lung cancer cells depleted of *RB1* is also associated with elevated markers of apoptosis and mitotic arrest (Fig. 7C). Similarly, natural RB1 loss in MDA-MB-361PR cells is associated with elevated BUBR1 and MAD2, but not MYC, levels and, in response to LY3295668, stabilized cyclin B1 and increased apoptosis (Fig. 7D and E; Supplementary Fig. S15). Together, these data suggest a unifying model (Fig. 7F) in which AURKA can promote mitotic exit despite an activated SAC. This function, which presumably requires higher levels of catalytic activity than the various functions of AURKA in mitotic entry and is therefore more sensitive to AURKAi, is only vital to cells with mitotic stress caused by loss of RB1, MYC amplification, or spindle poisons such as tubulin inhibitors.

DISCUSSION

To date, no drugs specifically tailored to the prototypical TSG, *RB1*, have been discovered. Drug screens across large panels of cancer lines are, in principle, well suited for the discovery of novel "gene–drug" synthetic lethal relationships but have so far failed to identify strong candidates for *RB1*. Two large screens using conventional 72-hour assays (21, 22) did not report drugs with significantly enhanced activity toward *RB1*^{mut} cancer cells, although the Garnett et al. study (22) found a significant association between *RB1* mutation and resistance to both CDK4/6 and MEK inhibitors. Using an assay that corrects for the growth rate bias of conventional fixed duration assays, we report that, among a collection of 36 cell-cycle inhibitors, inhibitors of AURKA or AURKB show the strongest differential cytotoxicity toward *RB1*^{mut} versus wild-type cancers. A companion paper in this issue by Oser and colleagues describes a dependency of *RB1*-mutant cells on the *AURKB* gene and, in accord with our data, a corresponding sensitivity of *RB1*-mutant cells to inhibitors of either AURKA or AURKB kinase activities.

To establish that *RB1*-AURKAi synthetic lethality is indeed a consequence of AURKA inhibition, we introduce and use LY3295668, a new, truly specific AURKAi, and show that LY3295668 cytotoxicity toward *RB1*^{mut} cells is counteracted by a drug-binding defective AURKA variant. We have followed modern usage (47, 48) in using the term "synthetic lethality" to describe a gene–drug interaction: the effect of concomitant inhibitory perturbations to the *RB1* gene and the AURKA function. Interestingly, despite surviving high concentrations of AURKA inhibitors, *RB1*–wild-type cells do not appear to tolerate knockout of the *AURKA* gene, which is essential in mammalian cells (23–25). Therefore, this appears to represent an example where protein depletion has a more severe phenotype than enzyme inhibition (6), and hence there is no evidence of a corresponding *RB1–AURKA* gene–gene synthetic lethality. Such a discrepancy could be caused if AURKA has important, kinase-independent functions (49).

The model we propose (Fig. 7F) to explain the striking sensitivity of *RB1*-mutant cells to AURKAi is premised on the unique role of high-level AURKA kinase activity in overriding an activated SAC (44, 45), a function that is likely distinct from the essential functions of AURKA in normal mitosis. On the basis of prior reports showing that RB1 loss is associated with increased priming of the SAC (12, 13, 43), we hypothesize that *RB1*-mutant, but not *RB1* wild-type, cells constitutively require this function of AURKA to exit mitosis. The model invokes an evolutionary process. It is well established that RB1 loss, by itself, can be detrimental to mammalian cells, and an unknown mitotic escape mechanism has been postulated to necessarily occur during the evolution of RB1 loss in cancer cells to compensate for the fitness disadvantage otherwise incurred (13). Our hypothesis is that loss of *RB1* function imparts a fitness advantage on cancer cells only if AURKA kinase activity is sufficiently high to overcome a mitotic delay. By examining a model of natural evolution of RB1 loss in the context of resistance to CDK4/6i, we have been able to begin to test this hypothesis. We show that cells that lose RB1 as a mechanism of resistance to the CDK4/6i palbociclib show increased BUBR1 and MAD2 and are sensitized to AURKAi cytotoxicity.

Future work will be necessary to rigorously test and refine our model. It will also be important to further tease apart the relative contributions of MYC proteins and RB1 loss to AURKAi sensitivity. *RB1* loss and *MYC* amplification commonly co-occur, especially in SCLC, and we have not been able to identify *RB1*-mutant cells that do not coexpress a MYC protein to completely rule out a role for MYC in the synthetic lethal effect. Indeed, MYC proteins may play an essential role in cells with defective RB1, necessitating expression of at least one MYC family member in RB1-null cells (50). However, we have been able to show (i) that *RB1*^{mut} SCLC is more sensitive than *RB1*^{WT} SCLC, despite similar expression levels of MYC proteins, both *in vitro* and *in vivo*; (ii) that artificial *RB1* depletion by three

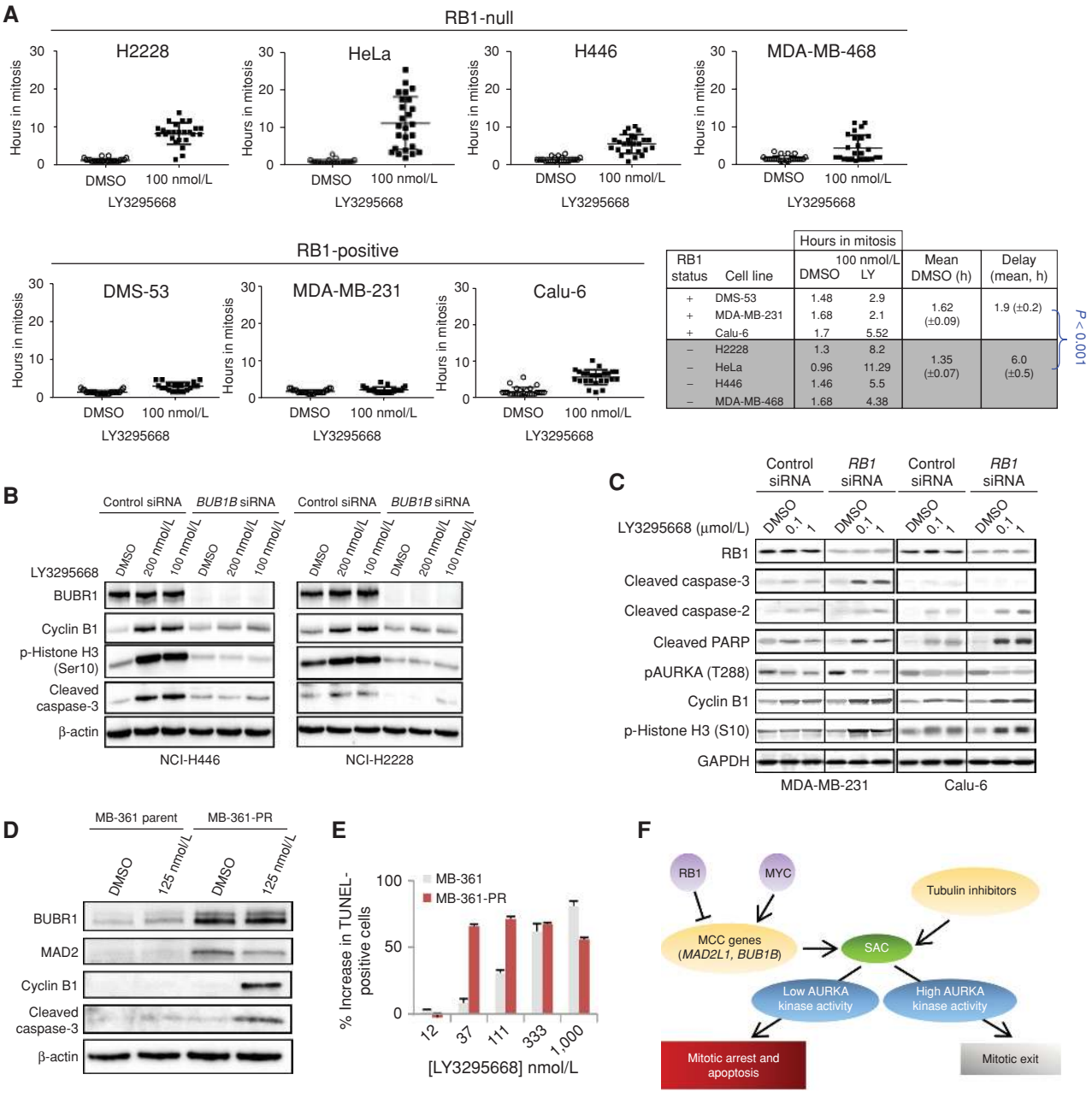

RB1 status	Cell line	Hours in mitosis DMSO	Hours in mitosis 100 nmol/L LY	Mean DMSO (h)	Delay (mean, h)
+	DMS-53	1.48	2.9	1.62 (±0.09)	1.9 (±0.2)
+	MDA-MB-231	1.68	2.1		
+	Calu-6	1.7	5.52		
–	H2228	1.3	8.2	1.35 (±0.07)	6.0 (±0.5)
–	HeLa	0.96	11.29		
–	H446	1.46	5.5		
–	MDA-MB-468	1.68	4.38		

$P < 0.001$

Figure 7. Cytotoxicity and mitotic arrest of RB1-null cells by AURKAi requires SAC function. **A,** Duration in mitosis was determined from IncuCyte imaging data for 4 RB1-null and 3 RB1–positive cell lines treated with 100 nmol/L LY3295668 or DMSO. The table lists the mean duration for each cell line, and the aggregated mean duration and mean delay for the RB1-positive and RB1-null cells without treatment (DMSO) or LY-treated, respectively. Two-tailed $P < 0.0001$ for the difference in mean delay for the two groups. **B,** NCI-H446 or NCI-H2228 cells were transfected with *BUB1B* siRNA and treated for 24 hours with LY3295668 before lysis and immunoblotting with the indicated antibodies. **C,** *RB1* was depleted by siRNA followed by 48-hour treatment with LY3295668 before lysis and immunoblotting with the indicated antibodies. **D,** MB-361-PR and parental MB-361 cells were treated with DMSO or 125 nmol/L LY3295668 for 24 hours before lysis and immunoblotting with the indicated antibodies. **E,** The percentage of TUNEL-positive MB-361-PR and parental MB-361 cells treated with LY3295668 for 72 hours relative to DMSO from high content imaging in 2 independent experiments. **F,** Unifying model posits that cancers with a hypersensitive or "primed" SAC depend on AURKA for mitotic exit and survival. *RB1* mutation or loss can prime the SAC, explaining the *RB1*-AURKAi synthetic lethality reported in this study. Other perturbations that prime the SAC, such as tubulin inhibitors or *MYC* amplification, may also show increased dependence on AURKA kinase activity to escape mitosis and survive.

different methods (siRNA, shRNA, and CRISPR/Cas9), as well as (iii) natural selection of RB1 loss in response to CDK4/6i, in various RB1-positive cancer cells, can clearly sensitize to AURKAi without obvious increase in MYC protein levels. In fact, our model may help explain the association of MYC family genes with AURKAi because MYC has been reported to activate *MAD2L1* expression (43, 51). Other perturbations that prime the SAC would also be predicted to sensitize cells to AURKA. In this regard, we note that the potentiation of taxane cytotoxicity by dual AURKA/B has been attributed to AURKA (52). *AURKA* amplification, which is a frequent event in various epithelial tumors (53), was not associated with AURKAi hypersensitivity in our profiling, perhaps because it is a vestige of adaptation to an SAC primed by a perturbation no longer present, such as from prior cytotoxic chemotherapy.

In summary, the data presented here predict that truly specific AURKAi will provide a better therapeutic window than classic cytotoxic agents for the treatment of $RB1^{mut}$ malignancies, permitting more aggressive dosing regimens. The poor prognosis of patients whose cancers lack functional RB1, coupled with the recent descriptions of *RB1* mutations in cancers that become resistant to inhibitors of EGFR (9) and CDK4/6 (11), highlights the pressing need for more effective treatments directed toward this tumor suppressor. To this end, a clinical trial is under way to test continuous dosing of LY3295668 for the treatment of patients with RB1-deficient cancers (NCT03092934).

METHODS

Cell Lines

All cell lines were obtained from commercial vendors and were cultured in conditions recommended by vendors. Cell line histology and site of origin annotation was derived from the source vendor or the Catalogue of Somatic Mutations in Cancer (COSMIC) cancer cell line database (www.cancer.sanger.ac.uk). Prior to use, cell lines were tested for *Mycoplasma* using a PCR-based method, and cell line authenticity was confirmed by STR-based DNA finger printing and multiplex PCR (IDEXX-Radil). For *Mycoplasma*-free cultures with authentic STR fingerprints, growth curves were determined to establish average population doubling time in the absence of drug treatment for each cell line. Cell density was optimized to ensure robust, logarithmic cell growth for the duration of compound exposure. All cell lines were used within 10 passages after recovery.

Cell Proliferation Assays

The 2DT cell panel screening assays using CellTiter-Glo (CTG; Promega Corporation) and IC_{50} determinations were performed as previously described (19). For BM cell assays, human bone marrow mononuclear cells (AllCells LLC) were prepared according to the manufacturer's recommendations. BM cells were carefully thawed and suspended in warm growth media. The cells were resuspended the next day in media with human growth factors (erythropoietin, GM-CSF, IL3, and SCF/c-KIT ligand) and cultured for 72 hours. Then, the cells were seeded into 96-well plates and treated with DMSO control or various compounds for 48 hours before cell viability (CTG assay) was determined. In parallel, NCI-H446 cells (SCLC) were cultured and treated with DMSO control and various compounds for 48 hours before cell proliferation was measured.

High Content Imaging and Apoptosis Assays

To measure apoptosis by high content imaging, cells were fixed in 3.7% formaldehyde (Sigma, cat #F-1268) or Prefer (Anatech), permeabilized with 0.1% Triton X-100 (Sigma) in PBS (Gibco) for 10 minutes, washed several times with PBS and blocked with 1% bovine serum albumin (BSA; Invitrogen #15260-037) in PBS for 1 hour at room temperature. All subsequent dilutions and washes were performed in PBS. Cells were incubated with primary antibodies to cleaved caspase-3 (Cell Signaling Technology; #9661, RRID:AB_2341188) and cyclin B1 (BD Pharmingen; #554177, RRID:AB_395288) diluted in 1% BSA overnight at 4°C. Cells were then washed 3 times and incubated with secondary antibody, 5 μg/mL goat α-rabbit-Alexa-647 (Molecular Probes; #A-21244, RRID:AB_141663), and 200 ng/mL Hoechst 33342 (Molecular Probes; #21492) or DAPI (Sigma) to detect nuclear material for 1 hour at room temperature. Cells were washed again 3 times and imaged using a CellInsight NXT (Thermo Scientific) or Acumen eX3 (TTP Labtech Ltd). For CellInsight NXT, a minimum of 1,500 individual cellular images or 20 fields were captured for each well. Analysis was performed using the TargetActivation V.4 Bioapplication (Thermo Scientific). Arbitrary responder levels (percent positive for desired marker) were set based on the control groups for each cell line.

TUNEL staining was assayed with the In Situ Cell Death Detection, Fluorescein kit (Roche Applied Science) following the manufacturer's protocol. Fluorescence was captured using Acumen eX3.

To measure apoptosis by IncuCyte Zoom instrument (Essen BioScience), NCI-H446 and Calu-6 cells were plated on Costar 3596 plates and treated with LY3295668 at different concentrations for 24, 48, and 72 hours. Caspase 3/7 activation was measured with CellPlayer 96-Well Kinetic Caspase 3/7 reagent (Essen BioScience 4440). Green fluorescent images were acquired every 2 hours. Green objects counted (y-axis) were plotted against either real time (x-axis) or raw numbers as percent control.

RNA Interference Studies

Cell lines were grown overnight in the appropriate growth media recommended by ATCC. For *RB1* shRNA experiments, MDA-MB-231 and Calu-6 cells were transduced with *RB1* shRNA (TRCN194866 and TRCN196261) for 48 hours and treated with LY3295668 at the different concentrations for a further 48 hours. In addition, Calu-6 cells were also treated with MK5108 at different concentrations for 48 hours after *RB1* shRNA transduction. Cells were then stained with propidium iodide (PI) for 1 hour at room temperature. Fluorescence was read using Acumen eX3. For siRNA-mediated *RB1* knockdown in Calu-6 cells, cells were transfected with either Dharmacon *RB1* Smart Pool (cat #L-003296-00-0005) or nontargeting control (cat #D-001810-01-05) siRNA according to the manufacturer's protocol. Cells were then treated with DMSO or MK5108 at different concentrations. Cell growth was continuously measured using an ACEA instrument for 160 hours. For siRNA-mediated *MAD2L1* and *BUB1B* knockdown, NCI-H446 and NCI-H2228 cells were transfected with control siRNA2 (Ambion AM4637), *MAD2L1* (Ambion S20468, Dharmacon; cat #L-003271-00-0005), or *BUB1B* (Ambion S261, Dharmacon; cat #L-004101-00-0005) siRNA for 72 hours. Cells were then treated with DMSO, 100 nmol/L LY3295668, or 200 nmol/L LY3295668 for 24 hours.

shRNA Drug Modifier Screen

MDA-MB-468 and NCI-H446 cells were infected with the Module 1 Decipher library targeting the signaling pathways (Cellecta; cat #DHPAC-M1-P) at a multiplicity of infection of <1. The lentiviral-based library is composed of 5,043 genes with 5 to 6 plasmid pools per gene. Lentiviral particles were generated as described by the manufacturer. Infected cells were selected with puromycin for 72 hours. Following selection, cells were pooled, plated, and treated with DMSO or LY3295668 at IC_{90} concentration (200 nmol/L for MDA-MB-468 and 400 nmol/L for H446) for 6 (MDA-MB-468) or 4 (H446) days, refreshing media once during the experiment. Genomic DNA was extracted using the Qiagen kit (cat #13362) as described in the manual. The barcodes tagged to each shRNA were amplified by PCR and sequenced on

Illumina NextSeq 500 according to Cellecta's manual. "Common suppressors" of AURKA were identified as genes whose shRNA abundance was enriched in LY-treated cells relative to DMSO control–treated cells in both H446 and MDA-MB-468 cells (FDR < 0.5).

Western Immunoblots

Cells were washed with PBS and were then lysed in lysis buffer containing protease and phosphatase inhibitors (Thermo Scientific, 1861281). Protein concentrations were determined by Bio-Rad Protein Assay Reagent (50000002). Cell lysates were cleared of debris by centrifugation at 14,000 rpm for 10 minutes. Western blots were performed with antibodies directed to RB1 (Cell Signaling Technology; 9309, RRID:AB_823629), AURKA (R&D Systems; AF3295), AURKA pT288 (Cell Signaling Technology; 3079, RRID:AB_2061481), cl-caspase 3 (Cell Signaling Technology; 9661, RRID:AB_2341188), cl-PARP (Cell Signaling Technology; 9541, RRID:AB_331426), cyclin B1 (Cell Signaling Technology; 4138, RRID:AB_2072132 or 12231), MAD2 (BD Transduction Laboratories; 610679, RRID:AB_398006), BUBR1 (Bethyl Labs; A300-386A), phosphohistone H3 ser10 (Millipore; 06-570, RRID:AB_310177), C-MYC (Abcam; ab32072, RRID:AB_731658), N-MYC (Thermo Fisher; MA1-16638, RRID:AB_2235735), MYCL1 (R&D Systems; AF4050, RRID:AB_2282440), GAPDH (Cell Signaling Technology; 32233), and actin (Sigma; A5441, RRID:AB_476744). The images were captured with Odyssey (LI-COR) or Amersham Imager 600 using the manufacturer's protocol.

AURKA *and* RB1 *Overexpression Vectors and Transfection*

Wild-type and mutant T217D *AURKA* and wild-type full-length *RB1* constructs were cloned into pcDNA3.1 and, for *AURKA*, tagged on the N-terminus with a 3× FLAG tag. Cells were transfected with lipofectamine 2000 (Invitrogen; 11668-109), and selected with Geneticin for *AURKA* (Gibco, 10131-035) at 400 μg/mL. Cells were plated onto poly-D-lysine plates (Corning; 354640) and treated in duplicate with a dose curve of either DMSO or LY3295668 for 2 hours (*AURKA*) or MK5108 72 hours (*RB1*). For *RB1* expression in MDA-MB-436 cells, expression levels were robust for at least 96 hours. AURKA activity was measured with phospho-AURKA (Thr288) Assay kit (MSD, K150JCD) as described by the manufacturer. Proliferation was assessed by CellTiter 96 (Promega, 63580) 4 days after cells were grown in RPMI-1640 (Gibco, 11875-093) and 10% FBS (Hyclone, SH30071.03).

Live-Cell Imaging

Mitotic timing was determined by live-cell phase contrast imaging by IncuCyte using a 20× objective. Briefly, cells were plated in multiwell plates, treated with LY3295668, and imaged every 30 minutes for 72 hours. Time in mitosis was determined by first following cell round up and chromosome condensation as mitotic entry and then exit from mitosis by cell flattening and chromosome decondensation. Quantification was done by manually tracking 25 cells per cell line and treatment in ImageJ and time in mitosis was graphed as individual mitotic events with average hours in mitosis ± SD.

Confocal Microscopy for Mitotic Phenotype

Cells were treated for 24 hours in glass bottom chamber slides. Following treatment, cells were fixed in 4% paraformaldehyde in PBS for 20 minutes, permeabilized with 0.2% Triton X-100 in PBS for 5 minutes, and blocked with 1% BSA in PBS for 20 minutes. Cells were incubated with primary antibodies to pericentrin (ab4448; Abcam) and alpha-tubulin (T5168; Sigma) diluted in 1% BSA/PBS for 1 hour, washed 3 times with PBS, incubated with secondary antibodies goat anti-rabbit Alexa Fluor 568 (A11011; Thermo Fisher) and goat anti-mouse Alexa Fluor 633 (A21053; Thermo Fisher) and sytox green (S7020; Thermo Fisher) to detect DNA for 1 hour. Cells were washed 3 times with PBS and imaged on a Zeiss LSM880 confocal microscope using the 63 × 1.4 NA oil objective. Z stacks were taken of cells representative of cellular mitotic phenotypes. Maximum intensity projections are shown.

In Vivo *Studies*

All *in vivo* studies were performed according to the Institutional Animal Care and Use Protocols of the party or provider conducting the experiments. NCI-H69 cells were harvested, washed, and resuspended in a 1:1 mixture of serum-free media and Matrigel (BD Biosciences, 354234) prior to subcutaneous implantation (6×10^6 cells/mouse) in the rear flank of athymic nude female mice (Harlan; 7–8 weeks). The SCLC patient-derived tumor models (LXFS 615, LXFS 650, and LXFS 1129) were derived from surgical specimens from patients at Oncotest (Oncotest GmbH, Charles River Laboratories). Following their primary implantation into nude mice (passage 1, P1), the tumor xenografts were passaged until stable growth patterns established. Stocks of early-passage xenografts were frozen in liquid nitrogen according to the relevant SOP for subsequent compound testing. Tumors were implanted subcutaneously in the left flank and randomized when the volume reached 80 to 200 mm^3 to start compound treatment. Tumor volume was estimated by using the formula: $V = L*W^2*0.536$, where L = larger of measured diameter and W = smaller of perpendicular diameter. Ten animals were used per treatment group and 8 animals in the vehicle group. Standard-of-care (SOC): etoposide 30 mg/kg subcutaneously (s.c.) Q7D×4 plus cisplatin 3.2 mg/kg s.c. Q7D×4.

Resistant Cell Line Generation

MDA-MB-361 and MCF-7 ER^+ breast cancer cell lines were used to derive variants with acquired resistance to palbociclib. For MDA-MB-361 cells, palbociclib selection was performed with or without a prior mutagenesis step to increase the diversity of resistant mechanisms available for selection. For mutagenesis we adapted a published method (33). The mutagen N-Ethyl-N-nitrosourea (ENU; Sigma, N3385) was dissolved in DMSO at 50 mg/mL and stored in aliquots at −80°C. MDA-MB-361 cells were cultured in complete medium at an exponential growth rate when ENU was added at a concentration of 50 μg/mL for 16 hours. The cells were then washed 3 times with fresh medium, replated in complete medium, and allowed to expand for about 2 weeks under optimal conditions. After ENU exposure and recovery, cells were cultured in 96-well plates at 5,000 cells/well in complete media with graded concentrations of the respective inhibitors. Wells were observed for cell growth by visual inspection under an inverted microscope. Fresh medium was supplemented when medium color changed. When growth in a well occurred, cells were transferred to 24-well plates and expanded in the presence of the corresponding inhibitor concentration used in the screen. Palbociclib-resistant derivatives of MDA-MB-361 and MCF-7 cell lines were also developed without ENU mutagenesis. To generate these variants, cells at 50% to 60% confluence were treated with inhibitors at a concentration approximating the IC_{50} for cell growth for about 1 to 2 weeks. Cells were passaged when they grew to 80% confluence. Upon every passage, cells were left untreated overnight for attachment and then retreated with incrementally higher doses. This process was repeated several times until the cells were able to grow in the presence of drugs at a high concentration with no apparent off-target effects.

Variants that showed at least a 10-fold decreased sensitivity to palbociclib (i.e., >10-fold increase in palbociclib IC_{50}) were identified from these experiments leading to the palbociclib-resistant MCF7 cells (MCF7-PR) and two variants of MDA-MB-361 cells using either ENU mutagenesis (MDA-MB-361-PRENU) or the rising dose method (MDA-MB-361-PR).

Genomic Data

Gene mutation, copy-number, and expression data were compiled from public domain data sets from COSMIC (www.cancer.sanger.ac.uk) and the Cancer Cell Line Encyclopedia (CCLE; www.broadinstitute.org/ccle/home).

Statistical Analysis

Statistical analysis of the cell panel screening results was conducted as previously described (19). Linear regression and one-way ANOVA models were applied to test the significance of the association between abemaciclib potency across the cell panel and gene expression and mutation, respectively. Abemaciclib IC_{50} was modeled on a log scale, and a generalized Tobit model was applied to account for censored IC_{50} data. FDR was computed using the Benjamini–Hochberg method.

Disclosure of Potential Conflicts of Interest

J. Du has ownership interest (including stock, patents, etc.) in Eli Lilly and Company. R.D. Van Horn has ownership interest (including stock, patents, etc.) in Eli Lilly and Company. A.M. Mc Nulty is a researcher at Eli Lilly and Company and has ownership interest (including stock, patents, etc.) in the same. M. Dowless has ownership interest in Eli Lilly stock. S.W. Eastman has ownership interest in Eli Lilly stock. M.Z. Dieter has ownership interest in Lilly Restricted Stock Units. H.-R. Qian has ownership interest (including stock, patents, etc.) in Eli Lilly and Company. G.D. Plowman was a Director on the Board of AURKA Pharma, Inc., is VP of Oncology Research at Eli Lilly, and has ownership interest (including stock, patents, etc.) in Eli Lilly. C. Reinhard has ownership interest (including stock, patents, etc.) in Eli Lilly. R.M. Campbell is a Research Fellow at Eli Lilly and Company and has ownership interest (including stock, patents, etc.) in the same. J.R. Henry has ownership interest (including stock, patents, etc.) in Eli Lilly. S.G. Buchanan has ownership interest (including stock, patents, etc.) in Eli Lilly and Company. No potential conflicts of interest were disclosed by the other authors.

Authors' Contributions

Conception and design: X. Gong, J. Du, S.H. Parsons, F.F. Merzoug, P.W. Iversen, B. Han, M. Dowless, M.J. Lallena, Y.-H. Hui, X.S. Ye, D.A. Barda, G.D. Plowman, C. Reinhard, R.M. Campbell, J.R. Henry, S.G. Buchanan

Development of methodology: X. Gong, J. Du, S.H. Parsons, F.F. Merzoug, L.-C. Chio, B. Han, S. Yao, H. Bian, C. Ficklin, L. Fan, D. Manglicmot, A. Pustilnik, M. Dowless, S. Chu, X.S. Ye, D.A. Barda, S.G. Buchanan

Acquisition of data (provided animals, acquired and managed patients, provided facilities, etc.): J. Du, S.H. Parsons, F.F. Merzoug, L.-C. Chio, R.D. Van Horn, X. Lin, W. Blosser, B. Han, S. Jin, H. Bian, C. Ficklin, L. Fan, A. Kapoor, A.M. Mc Nulty, K. Weichert, S.R. Wasserman, M. Dowless, C. Marugán, C. Baquero, S.W. Eastman, M.Z. Dieter, S. Chu, G.D. Plowman

Analysis and interpretation of data (e.g., statistical analysis, biostatistics, computational analysis): X. Gong, J. Du, S.H. Parsons, F.F. Merzoug, Y. Webster, P.W. Iversen, R.D. Van Horn, B. Han, S. Yao, C. Ficklin, S. Antonysamy, K. Froning, K. Weichert, S.R. Wasserman, C. Marugán, C. Baquero, Y.-H. Hui, M.Z. Dieter, T. Doman, S. Chu, H.-R. Qian, X.S. Ye, S.G. Buchanan

Writing, review, and/or revision of the manuscript: X. Gong, J. Du, S.H. Parsons, F.F. Merzoug, Y. Webster, P.W. Iversen, R.D. Van Horn, S. Antonysamy, Y.-H. Hui, M.Z. Dieter, H.-R. Qian, X.S. Ye, D.A. Barda, G.D. Plowman, C. Reinhard, R.M. Campbell, J.R. Henry, S.G. Buchanan

Administrative, technical, or material support (i.e., reporting or organizing data, constructing databases): S.H. Parsons, X. Lin, W. Blosser, D. Manglicmot, M.Z. Dieter, H.-R. Qian, S.G. Buchanan

Study supervision: X. Gong, J. Du, F.F. Merzoug, X.S. Ye, G.D. Plowman, C. Reinhard, S.G. Buchanan

Other (served as a nonsalaried board member on AURKA Pharma and was involved as an advisor in the external clinical development of the compound described in the manuscript): G.D. Plowman

Acknowledgments

This research used resources of the Advanced Photon Source, a U.S. Department of Energy (DOE) Office of Science User Facility operated for the DOE Office of Science by Argonne National Laboratory under Contract No. DE-AC02-06CH11357. Use of the Lilly Research Laboratories Collaborative Access Team (LRL-CAT) beamline at Sector 31 of the Advanced Photon Source was provided by Eli Lilly Company, which operates the facility.

Received April 30, 2018; revised August 26, 2018; accepted October 24, 2018; published first October 29, 2018.

REFERENCES

1. Weinstein IB. Cancer. Addiction to oncogenes–the Achilles heal of cancer. Science 2002;297:63–4.
2. Muller FL, Colla S, Aquilanti E, Manzo VE, Genovese G, Lee J, et al. Passenger deletions generate therapeutic vulnerabilities in cancer. Nature 2012;488:337–42.
3. Kaelin WG Jr. The concept of synthetic lethality in the context of anticancer therapy. Nat Rev Cancer 2005;5:689–98.
4. Lord CJ, Tutt AN, Ashworth A. Synthetic lethality and cancer therapy: lessons learned from the development of PARP inhibitors. Annu Rev Med 2015;66:455–70.
5. Tsherniak A, Vazquez F, Montgomery PG, Weir BA, Kryukov G, Cowley GS, et al. Defining a cancer dependency map. Cell 2017;170:564–76e16.
6. Weiss WA, Taylor SS, Shokat KM. Recognizing and exploiting differences between RNAi and small-molecule inhibitors. Nat Chem Biol 2007;3:739–44.
7. Burkhart DL, Sage J. Cellular mechanisms of tumour suppression by the retinoblastoma gene. Nat Rev Cancer 2008;8:671–82.
8. Sherr CJ, McCormick F. The RB and p53 pathways in cancer. Cancer Cell 2002;2:103–12.
9. Niederst MJ, Sequist LV, Poirier JT, Mermel CH, Lockerman EL, Garcia AR, et al. RB loss in resistant EGFR mutant lung adenocarcinomas that transform to small-cell lung cancer. Nat Commun 2015;6:6377.
10. Musgrove EA, Sutherland RL. Biological determinants of endocrine resistance in breast cancer. Nat Rev Cancer 2009;9:631–43.
11. Condorelli R, Spring L, O'Shaughnessy J, Lacroix L, Bailleux C, Scott V, et al. Polyclonal RB1 mutations and acquired resistance to CDK 4/6 inhibitors in patients with metastatic breast cancer. Ann Oncol 2018;29:640–5.
12. Manning AL, Dyson NJ. RB: mitotic implications of a tumour suppressor. Nat Rev Cancer 2012;12:220–6.
13. Malumbres M. Oncogene-induced mitotic stress: p53 and pRb get mad too. Cancer Cell 2011;19:691–2.
14. Herrera-Abreu MT, Palafox M, Asghar U, Rivas MA, Cutts RJ, Garcia-Murillas I, et al. Early adaptation and acquired resistance to CDK4/6 inhibition in estrogen receptor-positive breast cancer. Cancer Res 2016;76:2301–13.
15. Dean JL, Thangavel C, McClendon AK, Reed CA, Knudsen ES. Therapeutic CDK4/6 inhibition in breast cancer: key mechanisms of response and failure. Oncogene 2010;29:4018–32.
16. Zhao J, Zhang Z, Liao Y, Du W. Mutation of the retinoblastoma tumor suppressor gene sensitizes cancers to mitotic inhibitor induced cell death. Am J Cancer Res 2014;4:42–52.
17. Peng SB, Henry JR, Kaufman MD, Lu WP, Smith BD, Vogeti S, et al. Inhibition of RAF isoforms and active dimers by LY3009120 leads to anti-tumor activities in RAS or BRAF mutant cancers. Cancer Cell 2015;28:384–98.
18. Robinson TJ, Liu JC, Vizeacoumar F, Sun T, Maclean N, Egan SE, et al. RB1 status in triple negative breast cancer cells dictates response to radiation treatment and selective therapeutic drugs. PLoS One 2013;8:e78641.
19. Gong X, Litchfield LM, Webster Y, Chio LC, Wong SS, Stewart TR, et al. Genomic aberrations that activate D-type cyclins are associated with enhanced sensitivity to the CDK4 and CDK6 inhibitor abemaciclib. Cancer Cell 2017;32:761–76e6.

20. Fallahi-Sichani M, Honarnejad S, Heiser LM, Gray JW, Sorger PK. Metrics other than potency reveal systematic variation in responses to cancer drugs. Nat Chem Biol 2013;9:708–14.
21. Barretina J, Caponigro G, Stransky N, Venkatesan K, Margolin AA, Kim S, et al. The Cancer Cell Line Encyclopedia enables predictive modelling of anticancer drug sensitivity. Nature 2012;483:603–7.
22. Garnett MJ, Edelman EJ, Heidorn SJ, Greenman CD, Dastur A, Lau KW, et al. Systematic identification of genomic markers of drug sensitivity in cancer cells. Nature 2012;483:570–5.
23. Blomen VA, Majek P, Jae LT, Bigenzahn JW, Nieuwenhuis J, Staring J, et al. Gene essentiality and synthetic lethality in haploid human cells. Science 2015;350:1092–6.
24. Wang T, Birsoy K, Hughes NW, Krupczak KM, Post Y, Wei JJ, et al. Identification and characterization of essential genes in the human genome. Science 2015;350:1096–101.
25. Hart T, Chandrashekhar M, Aregger M, Steinhart Z, Brown KR, MacLeod G, et al. High-resolution CRISPR screens reveal fitness genes and genotype-specific cancer liabilities. Cell 2015;163:1515–26.
26. Meyers RM, Bryan JG, McFarland JM, Weir BA, Sizemore AE, Xu H, et al. Computational correction of copy number effect improves specificity of CRISPR-Cas9 essentiality screens in cancer cells. Nat Genet 2017;49:1779–84.
27. Dees EC, Cohen RB, von Mehren M, Stinchcombe TE, Liu H, Venkatakrishnan K, et al. Phase I study of aurora A kinase inhibitor MLN8237 in advanced solid tumors: safety, pharmacokinetics, pharmacodynamics, and bioavailability of two oral formulations. Clin Cancer Res 2012;18:4775–84.
28. Boss DS, Witteveen PO, van der Sar J, Lolkema MP, Voest EE, Stockman PK, et al. Clinical evaluation of AZD1152, an i.v. inhibitor of Aurora B kinase, in patients with solid malignant tumors. Ann Oncol 2011;22:431–7.
29. Schoffski P, Besse B, Gauler T, de Jonge MJ, Scambia G, Santoro A, et al. Efficacy and safety of biweekly i.v. administrations of the Aurora kinase inhibitor danusertib hydrochloride in independent cohorts of patients with advanced or metastatic breast, ovarian, colorectal, pancreatic, small-cell and non-small-cell lung cancer: a multi-tumour, multi-institutional phase II study. Ann Oncol 2015;26:598–607.
30. Amin M, Minton SE, LoRusso PM, Krishnamurthi SS, Pickett CA, Lunceford J, et al. A phase I study of MK-5108, an oral aurora a kinase inhibitor, administered both as monotherapy and in combination with docetaxel, in patients with advanced or refractory solid tumors. Invest New Drugs 2016;34:84–95.
31. Macarulla T, Cervantes A, Elez E, Rodriguez-Braun E, Baselga J, Rosello S, et al. Phase I study of the selective Aurora A kinase inhibitor MLN8054 in patients with advanced solid tumors: safety, pharmacokinetics, and pharmacodynamics. Mol Cancer Ther 2010;9:2844–52.
32. de Groot CO, Hsia JE, Anzola JV, Motamedi A, Yoon M, Wong YL, et al. A Cell Biologist's Field Guide to Aurora Kinase Inhibitors. Front Oncol 2015;5:285.
33. O'Hare T, Walters DK, Stoffregen EP, Jia T, Manley PW, Mestan J, et al. In vitro activity of Bcr-Abl inhibitors AMN107 and BMS-354825 against clinically relevant imatinib-resistant Abl kinase domain mutants. Cancer Res 2005;65:4500–5.
34. Bretones G, Delgado MD, Leon J. Myc and cell cycle control. Biochim Biophys Acta 2015;1849:506–16.
35. Brockmann M, Poon E, Berry T, Carstensen A, Deubzer HE, Rycak L, et al. Small molecule inhibitors of aurora-a induce proteasomal degradation of N-myc in childhood neuroblastoma. Cancer Cell 2013;24:75–89.
36. Mollaoglu G, Guthrie MR, Bohm S, Bragelmann J, Can I, Ballieu PM, et al. MYC drives progression of small cell lung cancer to a variant neuroendocrine subtype with vulnerability to Aurora kinase inhibition. Cancer Cell 2017;31:270–85.
37. Hook KE, Garza SJ, Lira ME, Ching KA, Lee NV, Cao J, et al. An integrated genomic approach to identify predictive biomarkers of response to the aurora kinase inhibitor PF-03814735. Mol Cancer Ther 2012;11:710–9.
38. Zhang J, Benavente CA, McEvoy J, Flores-Otero J, Ding L, Chen X, et al. A novel retinoblastoma therapy from genomic and epigenetic analyses. Nature 2012;481:329–34.
39. Pessina A, Albella B, Bayo M, Bueren J, Brantom P, Casati S, et al. Application of the CFU-GM assay to predict acute drug-induced neutropenia: an international blind trial to validate a prediction model for the maximum tolerated dose (MTD) of myelosuppressive xenobiotics. Toxicol Sci 2003;75:355–67.
40. Huang S, Holzel M, Knijnenburg T, Schlicker A, Roepman P, McDermott U, et al. MED12 controls the response to multiple cancer drugs through regulation of TGF-beta receptor signaling. Cell 2012;151:937–50.
41. Sivakumar S, Gorbsky GJ. Spatiotemporal regulation of the anaphase-promoting complex in mitosis. Nat Rev Mol Cell Biol 2015;16:82–94.
42. Schvartzman JM, Duijf PH, Sotillo R, Coker C, Benezra R. Mad2 is a critical mediator of the chromosome instability observed upon Rb and p53 pathway inhibition. Cancer Cell 2011;19:701–14.
43. Hernando E, Nahle Z, Juan G, Diaz-Rodriguez E, Alaminos M, Hemann M, et al. Rb inactivation promotes genomic instability by uncoupling cell cycle progression from mitotic control. Nature 2004;430:797–802.
44. Anand S, Penrhyn-Lowe S, Venkitaraman AR. AURORA-A amplification overrides the mitotic spindle assembly checkpoint, inducing resistance to Taxol. Cancer Cell 2003;3:51–62.
45. Katayama H, Wang J, Treekitkarnmongkol W, Kawai H, Sasai K, Zhang H, et al. Aurora kinase-A inactivates DNA damage-induced apoptosis and spindle assembly checkpoint response functions of p73. Cancer Cell 2012;21:196–211.
46. Hoar K, Chakravarty A, Rabino C, Wysong D, Bowman D, Roy N, et al. MLN8054, a small-molecule inhibitor of Aurora A, causes spindle pole and chromosome congression defects leading to aneuploidy. Mol Cell Biol 2007;27:4513–25.
47. Nijman SM. Synthetic lethality: general principles, utility and detection using genetic screens in human cells. FEBS Lett 2011;585:1–6.
48. Leung AW, de Silva T, Bally MB, Lockwood WW. Synthetic lethality in lung cancer and translation to clinical therapies. Mol Cancer 2016;15:61.
49. Toya M, Terasawa M, Nagata K, Iida Y, Sugimoto A. A kinase-independent role for Aurora A in the assembly of mitotic spindle microtubules in Caenorhabditis elegans embryos. Nat Cell Biol 2011;13:708–14.
50. Liu H, Tang X, Srivastava A, Pecot T, Daniel P, Hemmelgarn B, et al. Redeployment of Myc and E2f1-3 drives Rb-deficient cell cycles. Nat Cell Biol 2015;17:1036–48.
51. Menssen A, Epanchintsev A, Lodygin D, Rezaei N, Jung P, Verdoodt B, et al. c-MYC delays prometaphase by direct transactivation of MAD2 and BubR1: identification of mechanisms underlying c-MYC-induced DNA damage and chromosomal instability. Cell Cycle 2007;6:339–52.
52. Scharer CD, Laycock N, Osunkoya AO, Logani S, McDonald JF, Benigno BB, et al. Aurora kinase inhibitors synergize with paclitaxel to induce apoptosis in ovarian cancer cells. J Transl Med 2008;6:79.
53. Bischoff JR, Plowman GD. The Aurora/Ipl1p kinase family: regulators of chromosome segregation and cytokinesis. Trends Cell Biol 1999;9:454–9.